International Journal of Microwave and Wireless Technologies

cambridge.org/mrf

A 4 × 4 Butler matrix with switching/steering beams based on new tunable phase difference couplers

Taleb Mohamed Benaouf[1], Abdelaziz Hamdoun[2], Mohamed Himdi[3], Olivier Lafond[3] and Hassan Ammor[1]

[1]ERSC, Mohammadia School of Engineers, Mohammed V University of Rabat, Rabat, Morocco; [2]XLIM Lab UMR CNRS 7252, University of Poitiers, Angoulême, France and [3]Institut d'Electronique et des Technologies du numeRique (IETR), UMR CNRS 6164, Université de Rennes, Rennes, France

Research Paper

Cite this article: Benaouf TM, Hamdoun A, Himdi M, Lafond O, Ammor H (2024) A 4 × 4 Butler matrix with switching/steering beams based on new tunable phase difference couplers. *International Journal of Microwave and Wireless Technologies* **16**(6), 1033–1042. https://doi.org/10.1017/S175907872300154X

Received: 21 July 2023
Revised: 29 November 2023
Accepted: 1 December 2023

Keywords:
antenna; beamforming; Butler Matrix; continuous tunability; reconfigurable 3dB coupler; wireless application

Corresponding author:
Taleb Mohamed Benaouf;
Email: benaouf@research.emi.ac.ma

Abstract

Basically, a 4 × 4 Butler matrix (BM) connected to an antenna array allows to have four beams, each oriented in a specific direction depending on the excitation port. In this paper, an almost continuously steerable beam system based on a conventional 4 × 4 BM with adjustable phase shift is presented and demonstrated. Here, varicap diodes are used instead of an additional phase shifter. Under different bias levels applied to the couplers throughout these varicap diodes, an output variable phase difference was obtained. A prototype of the proposed tunable BM integrated with an antenna array operating at 3.5 GHz was fabricated and tested. The experimental results show a good agreement with those simulated. A reflection and isolation coefficient better than −15 dB over the entire desired frequency band and an amplitude imbalance lower than ±1.5 dB were achieved. The measured radiating beam under different DC biasing can be oriented from ±6° to ±18° when port 1 or 4 is excited and oriented from ±32° to ±43° for ports 2 and 3.

Introduction

Beamforming is a signal processing technique to send or receive directional signals. The idea is to combine radiation elements in an array in such a way as to create constructive interference for signals at desired angles and destructive interference for the rest of the signals. This technique has become the core technology in modern mobile communication systems, which are developing rapidly.

The Blass [1], Nolen [2], and Butler matrices [3] are famous analog solutions that provide multibeams through the alternative selection of the input excitation. Between these, the Butler matrix (BM) has been implemented in most beam-switching array systems due to its straightforward use, low-loss nature, and easy implementation. The BM can be used in many applications, such as satellite applications [4], massive multi-input multi-output (MIMO) systems [5], and for sending and receiving data between several users [6].

A classical BM is a 2N × 2N network (N is an integer greater than or equal to 1). In a 2N × 2N BM, only 2N spatially orthogonal independent beams can be generated. For example, when N = 2, we will have the best-known 4 × 4 BM, consisting of four couplers, two crossovers, and two phase shifters, along with four input and output ports. By exciting one of the input ports, four signals with equal amplitudes and a phase difference of ±45° or ±135° will be generated at the output ports [4]. Thus, we can produce four different radiating beams when the 4 × 4 BM is associated with an antenna array. However, with the emergence of the Internet of Things and 5G technology, more channel capacity is required. Increasing the number of beams by adopting higher-order Butler arrays (N = 8, 16,...), could be a solution. Nevertheless, the number of couplers, crossovers, and phase shifters increases considerably when the number of beams increases, which results in the circuit size, higher transmission loss, and greater complexity of the circuit design. To reduce design complexity, several efforts have been reported [7–15]. These efforts can be divided into two categories. The first category consists in reducing or avoiding the use of crossovers. For example, a BM based on double-layer structure [7, 8], or the use of multilayer Complementary Metal Oxide Semiconductor (CMOS) technology [9]. The second one consists in eliminating, in terms of appearance, phase shifters by integrating them with couplers. For example, by using couplers with quasi-arbitrary phase differences [10, 11], one can have a BM without phase shifters [8]. The abovementioned studies eliminate phase shifters or crossovers, but the number of couplers remains the same as those in the conventional BM. Other studies have focused on improving the capacity while keeping the order of the matrix [12–15]. These studies are based on the application of additional phase shifting devices. In [12], phase reconfigurable synthesized transmission lines connected to the outputs of a 4 × 4 BM were reported. In a few other studies [13–15], additional phase shifters are integrated with the BM structure instead of placing them at the output ports. These extra phase shifters could be beneficial in increasing the beam's pointing angle range, usually at the expense of design complexity and additional power loss. However, it would not improve the intrinsic properties of the matrix. Furthermore, another study focused on reconfigurable directional couplers that are used in a BM system is reported in [16, 17], here the author relied on double section couplers with six positive intrinsic negative (PIN) diodes for each coupler, which causes design complexity with high cost. In this paper, a 4 × 4 BM based on couplers with a continuously variable output phase difference is presented. The characteristics of the proposed BM allow a better spatial coverage compared to the conventional 4 × 4 BM while avoiding to increase circuit size and design complexity. The theoretical design analysis of the proposed 4 × 4 BM is presented and discussed. To verify the proposed design, a 4 × 4 BM for 3.5 GHz applications is fabricated and measured. To validate the performance of the beam steering over a wide spatial coverage, the integration of the proposed BM along with a planar antenna array is presented.

Design and analysis

Couplers with a tunable phase difference present more challenges than those with a tunable frequency or power division ratio, as reflected by the limited studies in research articles. For the first time, a 3-dB coupler offering a continuously tunable phase difference was achieved using a tunable phase shifting unit [18]. Enhancements in bandwidth were attained by inserting a phase-tunable transmission line between the branch line segments, as described in [19]. To achieve a phase adjustment span of 180°, in [20] a design that integrates two tunable units, comprising open/short stubs and varactors, between the coupled lines was reported. The main advantage of our proposed tunable coupler based on varicap diodes is its simplicity, ease of manufacture, and low cost.

Coupler design

Figure 1 shows a conventional coupler and its equivalent model. Each branch of the coupler is represented by its Pi-network circuit equivalent [21]. To calculate the impedance Z_2 and electrical length θ_2 of the coupler from its equivalent circuit, the equations already obtained in [21] are required:

$$\frac{C_0}{2} = \frac{\tan\left(\frac{\theta_2}{2}\right)}{Z_2\omega} \tag{1}$$

$$L_2 = \frac{Z_2 \sin(\theta_2)}{\omega} \tag{2}$$

The proposed coupler consists in adding two variable capacitors to each of the two vertical branches, as shown in Fig. 2. This will provide a new electrical length and impedance. Note that the couple (θ, Z) and (θ', Z) are the new electrical lengths and impedance, respectively, of the left and right vertical branches of the proposed coupler after adding the variable capacitors, C_1 and C_2. θ represents the branch with C_1, θ' is the branch with C_2, and Z is the same for both.

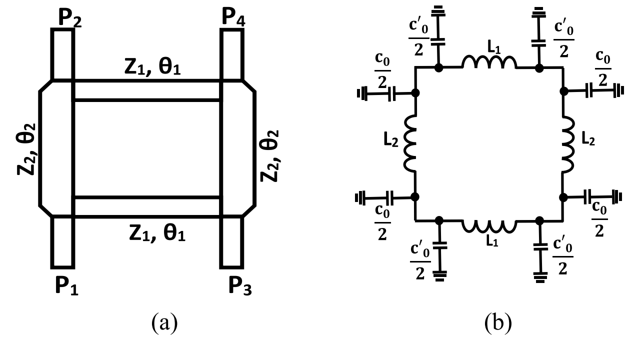

Figure 1. (a) Conventional coupler and (b) its equivalent in a Pi-network circuit.

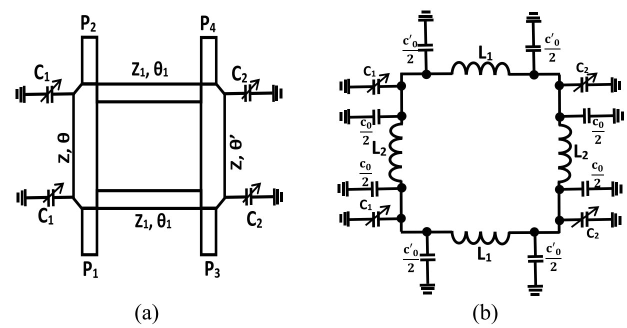

Figure 2. (a) The proposed coupler and (b) its equivalent in a Pi-network circuit.

To calculate θ and Z, it can be deducted from equations (1) and (2):

$$\frac{C_x}{2} = \frac{\tan\left(\frac{\theta}{2}\right)}{Z\omega} \tag{3}$$

$$L_x = \frac{Z \sin(\theta)}{\omega} \tag{4}$$

where C_x and L_x are, respectively, the equivalent capacitor and the inductance of the left branch after adding C_1.

Note that $C_x = C_1 + \frac{C_0}{2}$ and $L_x = L_2$. This allows writing equations (3) and (4) as follows:

$$\frac{C_1}{2} + \frac{C_0}{4} = \frac{\tan\left(\frac{\theta}{2}\right)}{Z\omega} \tag{5}$$

$$L_2 = \frac{Z \sin(\theta)}{\omega} \tag{6}$$

Replacing C_0 and L_2 by their values in equations (1) and (2):

$$\frac{C_1}{2} + \frac{\tan\left(\frac{\theta_2}{2}\right)}{2z_2\omega} = \frac{\tan\left(\frac{\theta}{2}\right)}{Z\omega} \tag{7}$$

$$\frac{Z_2 \sin(\theta_2)}{\omega} = \frac{Z \sin(\theta)}{\omega} \tag{8}$$

from equations (7) and (8), it can be deducted as follows:

$$\theta = 2\tan^{-1}\left[\frac{Z\omega C_1}{2} + \frac{Z}{2Z_2}\tan\left(\frac{\theta_2}{2}\right)\right] \tag{9}$$

$$Z = \frac{Z_2 \sin(\theta_2)}{\sin(\theta)} \tag{10}$$

https://doi.org/10.1017/S175907872300154X Published online by Cambridge University Press

where Z_2 is the impedance before adding the variable capacitors, $Z_2 = 35{,}35\ \Omega$.

To calculate the electrical length of the right vertical branch θ', simply replace C_1 with C_2 in equation (9).

Once the electrical lengths θ and θ' have been determined according to the added variable capacitors, it will be necessary to proceed with the analysis in even–odd mode to obtain the parameters of the proposed coupler. For this purpose, we can reuse all the results obtained after the analysis of the odd–even mode in [8, 9], precisely the closed-form equations:

$$P = \left|\frac{S_{21}}{S_{41}}\right| \tag{11}$$

$$\psi = \angle S_{41} - \angle S_{21} \tag{12}$$

P and ψ are, respectively, the power division ratio and the phase difference between the output ports. Port 1 is chosen as the input, 2 and 4 are the output ports, and port 3 is the isolated one.

$$Z_1 = Z_0 P\,|\sin\psi| \tag{13}$$

$$Z = \frac{Z_0 P\,|\sin\psi|}{\sqrt{1 + P^2 \sin^2\psi}} \tag{14}$$

where Z_0 and Z_1 are, respectively, the input impedance and the impedance of the two horizontal branches, with $Z_0 = Z_1 = 50\ \Omega$.

$$\theta_1 = \frac{\pi}{2} \tag{15}$$

$$\theta + \theta' = \pi \tag{16}$$

$$\theta = \tan^{-1}\left(\frac{Z_0 \tan\psi}{Z_1}\right) \tag{17}$$

$$\theta' = \pi - \tan^{-1}\left(\frac{Z_0 \tan\psi}{Z_1}\right) \tag{18}$$

Since $Z_0 = Z_1$, equation (17) can be simplified as:

$$\psi = \theta \tag{19}$$

Since $\psi = \theta$, it is clear from equations (10) and (14) that Z will depend on the coupler's output phase difference ψ. For example, when $\psi = 90^\circ$ (classical case), Z will be equal to 35,36 Ω. Since the proposed coupler consists in having a variable output phase difference, Z will be fixed at 46 Ω after optimization, independently of the ψ value. More explanations are given later.

Equation (13) shows that to maintain a tolerable coupling coefficient P of -3 dB $\pm$ 0.5 dB where $Z_0 = Z_1 = 50\ \Omega$, the output phase difference ψ has to be limited to $90^\circ \pm 40^\circ$.

By replacing θ by its value in equation (9), equation (19) became:

$$\psi = 2\tan^{-1}\left[\frac{Z\omega c_1}{2} + \frac{Z}{2Z_2}\tan\left(\frac{\theta_2}{2}\right)\right] \tag{20}$$

Equation (20) shows that the output phase difference of the coupler depends mainly on C_1, with the other parameters remaining constant. Also, the values of capacitors C_2 depend on C_1 and are used to obtain the θ' required to satisfy the condition (18).

To control the two variable capacitors independently, two biasing voltages are required. At 3.5 GHz, the optimized values of θ_2

Table 1. Optimized parameters of the proposed coupler

Parameters	Initial values of a classical passive hybrid coupler	Optimized values after adding the capacitors
θ_1	90°	90°
θ_2	90°	79°
Z_0	50 Ω	50 Ω
Z_1	50 Ω	50 Ω
Z_2	35.35 Ω	–
Z	–	46 Ω

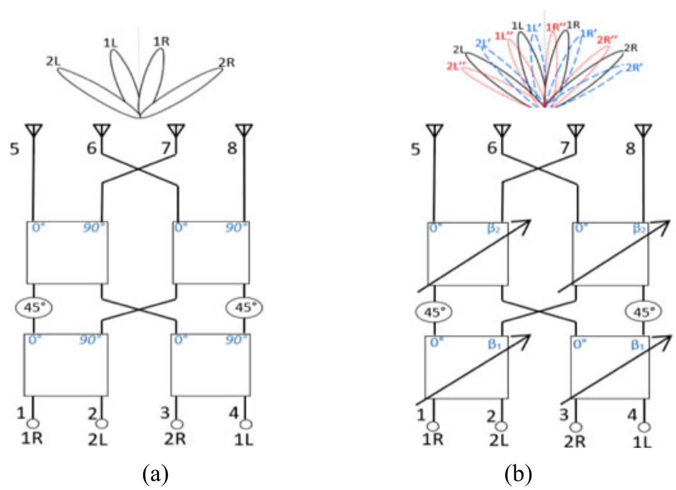

Figure 3. Schematic of (a) a conventional 4 × 4 Butler matrix and (b) the proposed 4 × 4 Butler matrix.

and Z_2, constituting the θ and Z of the proposed hybrid coupler, are, respectively, 79° and 46 Ω. These values have been optimized to keep having good performances of a classical 3-dB/90° hybrid coupler in terms of good matching, good isolation, and a good power ratio, while the phase shift is now ψ (see equation 20) instead of 90°. This optimization was validated by CST simulation software, and the values are shown in Table 1, while Fig. 2 illustrates the definitions of each parameter.

BM design

As a recall, a classic 4 × 4 BM has four input ports and four output ports (Fig. 3(a)). It consists of four 90° couplers, two 45° phase shifters, and two crossovers. When the BM is connected to an antenna array, it can provide four beams, each directed in a specific direction, as shown in Fig. 3(a). Comparing this conventional matrix with the 4 × 4 BM proposed in this work, as shown in Fig. 3(b), both matrices have the same structure, except that the proposed matrix allows having four beams, each of which can be oriented continuously in different directions. These directions are controlled by the voltages applied to the couplers.

Here, the proposed BM consists of two couplers with a phase difference of β_1, two couplers with a phase difference of β_2, two crossovers, and two 45° phase shifters. The input ports are denoted (1–4) and the output ports are (5–8), as presented in Fig. 3(b). Table 2 summarizes the phase responses obtained at the output ports and the corresponding excited input ports.

https://doi.org/10.1017/S175907872300154X Published online by Cambridge University Press

Table 2. The phase response of the proposed Butler matrix

	Input port			
Output port	P1	P2	P3	P4
P5	−45°	$-\beta_1$ −45°	$-\beta_2$	$-\beta_1$ $-\beta_2$
P6	$-\beta_1$	0°	$-\beta_1$ −45° $-\beta_2$	−45° $-\beta_2$
P7	−45° $-\beta_2$	$-\beta_1$ −45° $-\beta_2$	0°	$-\beta_1$
P8	$-\beta_1$ $-\beta_2$	$-\beta_2$	$-\beta_1$ −45°	−45°

The progressive phase differences $\Delta\theta$ between the output ports depending on the excitation case are obtained as follows:

Case 1: P1 excited

$$\Delta\theta_1 = \angle S_{61} - \angle S_{51} = \angle S_{71} - \angle S_{61} = \angle S_{81} - \angle S_{71} \tag{21}$$

$$\Delta\theta_1 = -\beta_1 + 45^\circ = -45^\circ - \beta_2 + \beta_1 = -\beta_1 + 45^\circ \tag{22}$$

Case 2: P2 excited

$$\Delta\theta_2 = \angle S_{62} - \angle S_{52} = \angle S_{72} - \angle S_{62} = \angle S_{82} - \angle S_{72} \tag{23}$$

$$\Delta\theta_2 = \beta_1 + 45^\circ = -\beta_1 - 45^\circ - \beta_2 = \beta_1 + 45^\circ \tag{24}$$

Case 3: P3 excited

$$\Delta\theta_3 = \angle S_{63} - \angle S_{53} = \angle S_{73} - \angle S_{63} = \angle S_{83} - \angle S_{73} \tag{25}$$

$$\Delta\theta_3 = -\beta_1 - 45^\circ = \beta_1 + 45^\circ + \beta_2 = -\beta_1 - 45^\circ \tag{26}$$

Case 4: P4 excited

$$\Delta\theta_4 = \angle S_{64} - \angle S_{54} = \angle S_{74} - \angle S_{64} = \angle S_{84} - \angle S_{74} \tag{27}$$

$$\Delta\theta_4 = -45^\circ + \beta_1 = -\beta_1 + 45^\circ + \beta_2 = -45^\circ + \beta_1 \tag{28}$$

From equations (21–28), it and can be deduced that $\Delta\theta$ depends on the value of β_1, and β_1 depends on β_2:

$$\Delta\theta_1 = -\beta_1 + 45^\circ \tag{29}$$

$$\Delta\theta_2 = \beta_1 + 45^\circ \tag{30}$$

$$\Delta\theta_3 = -\beta_1 - 45^\circ \tag{31}$$

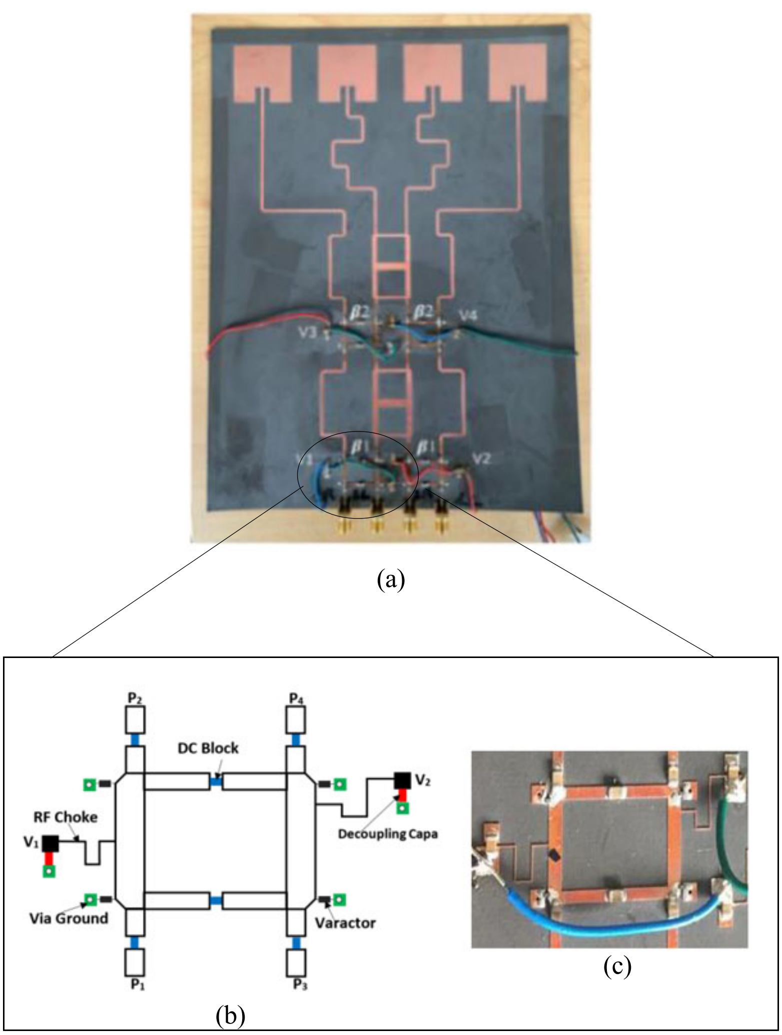

Figure 4. (a) Photograph of the fabricated BM integrated with a planar antenna array; (b) schematic diagram of the reconfigurable coupler; and (c) a zoom-in of the reconfigurable coupler.

https://doi.org/10.1017/S175907872300154X Published online by Cambridge University Press

Table 3. Required voltage for each configuration

		Phase difference of couplers outputs		Biasing voltages (V)				Phase difference of BM outputs
Configs	Ports	β_1	β_2	V_1	V_2	V_3	V_4	$\Delta\theta$
Config_1	P1	71°	52°	3.1	7	2.3	17	−26°
	P2	71°	52°	7	3.1	2.3	17	116°
	P3	71°	52°	3.1	7	17	2.3	−116°
	P4	71°	52°	7	3.1	17	2.3	26°
Config_2	P1	90°	90°	4.2	4.2	4.2	4.2	−45°
	P2	90°	90°	4.2	4.2	4.2	4.2	135°
	P3	90°	90°	4.2	4.2	4.2	4.2	−135°
	P4	90°	90°	4.2	4.2	4.2	4.2	45°
Config_3	P1	109°	128°	7	3.1	17	2.3	−64°
	P2	109°	128°	3.1	7	17	2.3	154°
	P3	109°	128°	7	3.1	2.3	17	−154°
	P4	109°	128°	3.1	7	2.3	17	64°

Note: BM = Butler matrix.

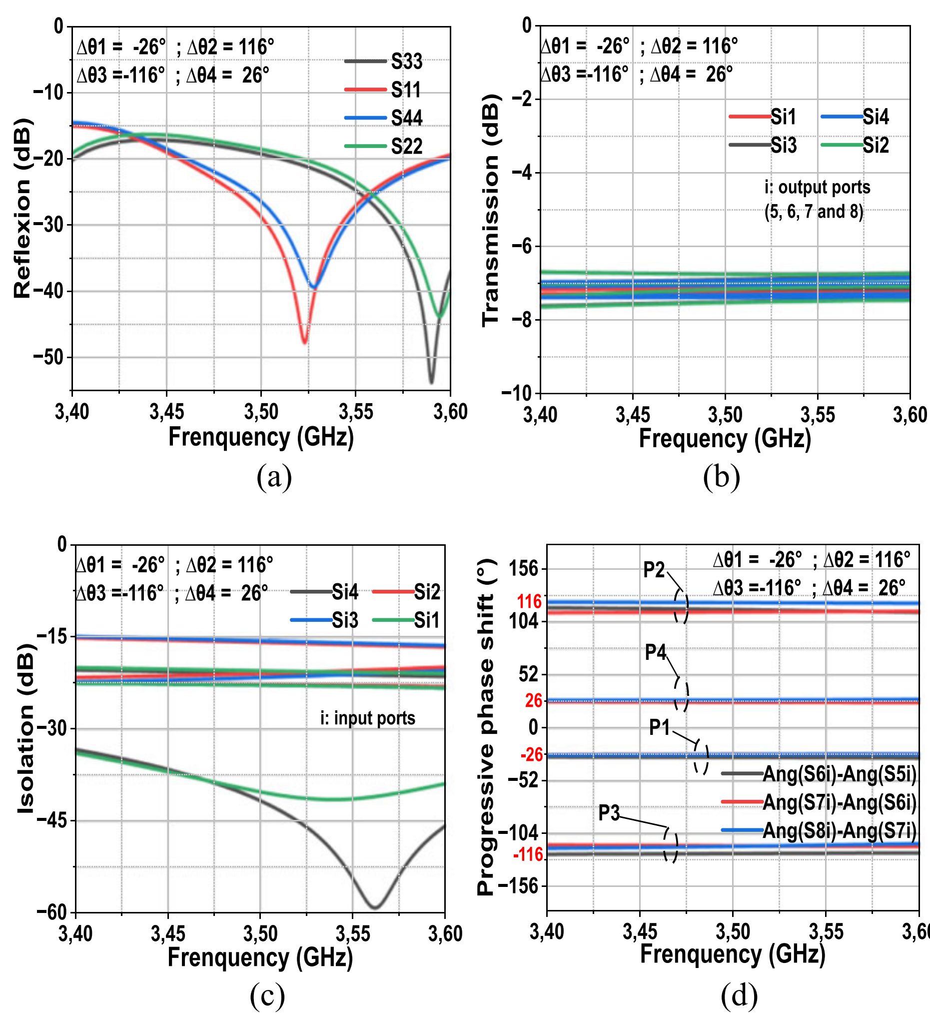

Figure 5. Simulated S-parameters and phase difference of the proposed Butler matrix for Config_1 when $\Delta\theta = \pm 26^{\circ}, \pm 116^{\circ}$.

https://doi.org/10.1017/S175907872300154X Published online by Cambridge University Press

$$\Delta\theta_4 = -45^\circ + \beta_1 \quad (32)$$

$$\beta_1 = 45^\circ + \frac{\beta_2}{2} \quad (33)$$

From equations (29–33), the case of the classical 4 × 4 matrix can be obtained when $\beta_1 = \beta_2 = 90^\circ$. The progressive phase differences between the output ports will therefore be $\pm 45^\circ$ and $\pm 135^\circ$.

Simulation and measurement results

To verify the design concept, a BM connected to an antenna array (half-wavelength distance between adjacent elements) by transmission lines operating at 3.5 GHz is designed and fabricated. Figure 4 shows a photograph of the prototype fabricated on a printed circuit board: Rogers RT5880 substrate with a thickness of 0.508 mm, a dielectric constant of 2.2, and a loss tangent of 0.0009.

A commercially available varactor MA46H120, from MACOM Technical Solutions, is used to provide tunability as it provides a capacitance tuning range from 0.165 pF to 1.23 pF at 3.5 GHz by adjusting the DC voltage from 0 to 19 V [22]. This allowed us to have a range of output phase differences from 52° to 128° while keeping a coupling factor of −3 dB (±0.5 dB).

Therefore, to clearly discuss the EM simulations as well as the measurement results, only three output phase shift difference values will be treated and analyzed. Here, the two extreme values (i.e., 52° and 128°) and one 90° allowing to have the conventional structure are chosen to conduct this analysis. Here, the following three configurations will be studied:

1. Config_1: when the phase difference is at its minimum value, $\beta_2 = 52^\circ$.
2. Config_2: when $\beta_2 = 90^\circ$, as already explained here, the conventional case is verified.
3. Config_3: when the phase difference is at its maximum value, $\beta_2 = 128^\circ$.

We can deduce from equation (33) that when $\beta_2 = 52^\circ$ (Config_1), $\beta_1 = 71^\circ$. When $\beta_2 = 90^\circ$ (Config_2), $\beta_1 = 90^\circ$. When $\beta_2 = 128^\circ$ (Config _3), $\beta_1 = 109^\circ$.

Table 3 shows in detail the value of β_1 regarding β_2 and the required voltage values for each phase difference.

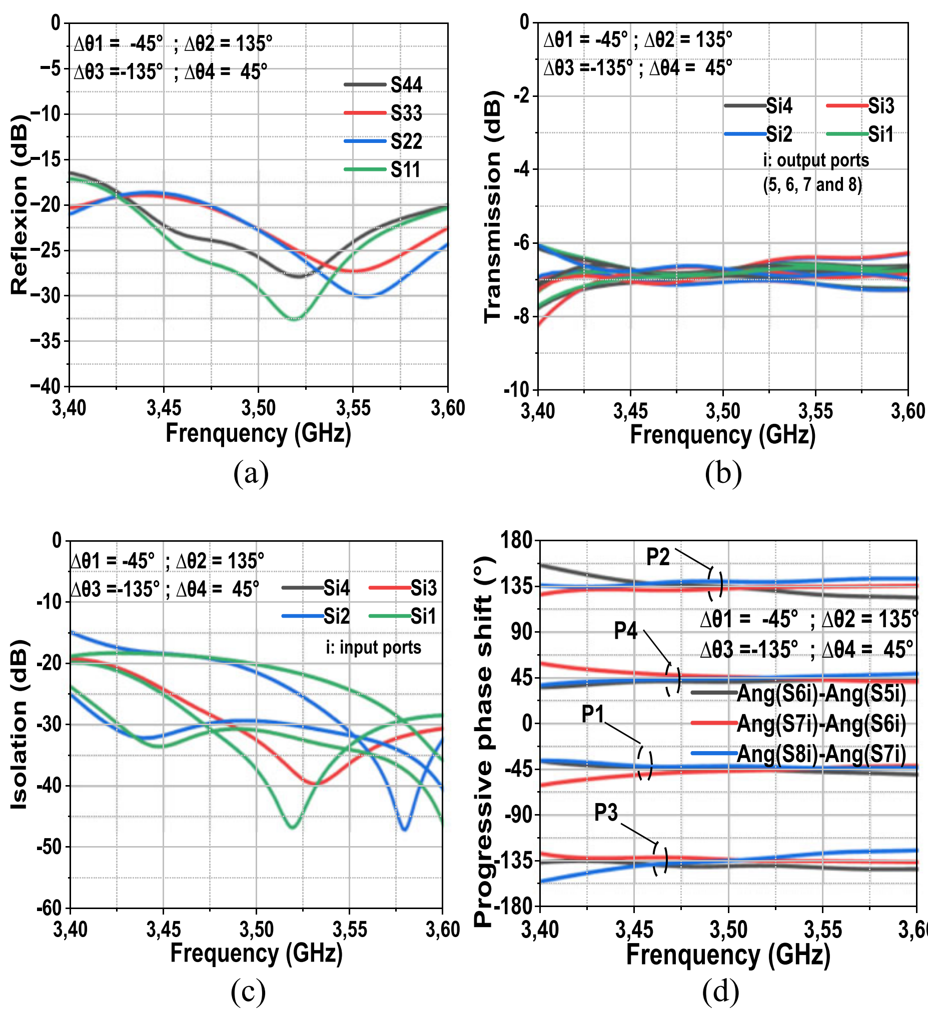

Figure 6. Simulated S-parameters and phase difference of the proposed Butler matrix for Config_2 (Conventional case) when $\Delta\theta = \pm 45^\circ$ and $\pm 135^\circ$.

https://doi.org/10.1017/S175907872300154X Published online by Cambridge University Press

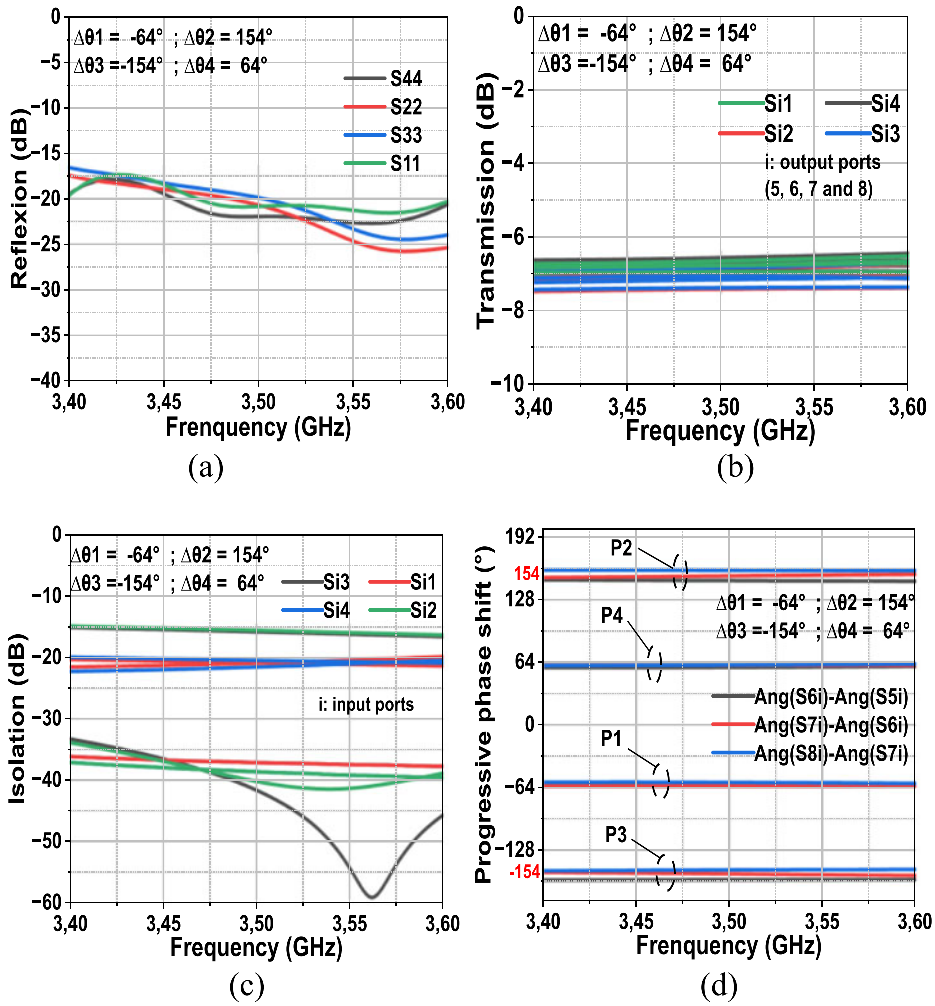

Figure 7. Simulated S-parameters and phase difference of the proposed Butler matrix for Config_3 when $\Delta\theta = \pm 64^{\circ}, \pm 154^{\circ}$.

BM

Unfortunately, it will not be possible to have the BM measurements without the antenna array since, in our prototype, they are connected by transmission lines, as shown in Fig. 4. We think it would not be very practical to fabricate another prototype since we can validate the principle of our work by measuring the radiation pattern at different control voltages.

The simulated results of S-parameter and phase difference are depicted in Figs. 5–7, respectively, for Config_1, Config_2, and Config_3. As can be observed, from 3.4 GHz to 3.6 GHz, the worst case of the insertion loss is about −7.7 dB and occurs for Config_1, while the reflection and the isolation are better than −15.5 dB at all ports for the three configurations.

The same figures illustrate the simulated progressive phase shift, and it is clearly noted that, as was expected, those values achieved are in great agreement with slight variations to what was theoretically expected. These variations are more seen for Config_1 from 3.40 GHz to 3.425 GHz, a little bit far for the working frequency of 3.5 GHz.

BM with antennas

To verify the radiation performance, a four-element patch linear antenna array is connected to the proposed BM. Each patch has a size of 29 mm × 29 mm, with a half-wavelength between adjacent patches. The comparison of the simulated and measured results of the radiation pattern of the three configurations is presented in Fig. 8(a–c). A good agreement between both simulation and measurement results can be noted, in particular for the beams obtained from the excitation of ports 1 and 4. A slight disagreement between simulations and measurements is observed and is varied between 0° and 4°, while it can reach 7° when the RF signal is from port 2 or 3. This could be due to the wires used for DC voltage and/or the misconnection (i.e., weld the connector) of the SMA connector at the different input ports.

As shown in Fig. 8(a), the beam directions in Config_1 are oriented at $\pm 6^{\circ}$ for ports 1 and 4, and at $\pm 26^{\circ}$ (simulated) and $\pm 32^{\circ}$ (measured) for ports 2 and 3. In the second configuration, Config_2, as can be seen in Fig. 8(b), the beams are oriented at $\pm 10^{\circ}$ when ports 1 and 4 are excited, and at $\pm 30^{\circ}$ (simulated) and $\pm 36^{\circ}$ (measured) when the signal is from ports 2 and 3.

Figure 8(c) shows the results of the radiation pattern of the third configuration, Config_3. It can be observed that the orientation of the beams obtained from ports 1 and 4 is at $\pm 14^{\circ}$ (simulated) and $\pm 18^{\circ}$ (measured), and at $\pm 36^{\circ}$ (simulated) and $\pm 43^{\circ}$ (measured) for ports 2 and 3.

According to Fig. 9, through all sets of measured curves of the three configurations, the three sequences of the beams directions related to each configuration can be easily distinguished.

https://doi.org/10.1017/S175907872300154X Published online by Cambridge University Press

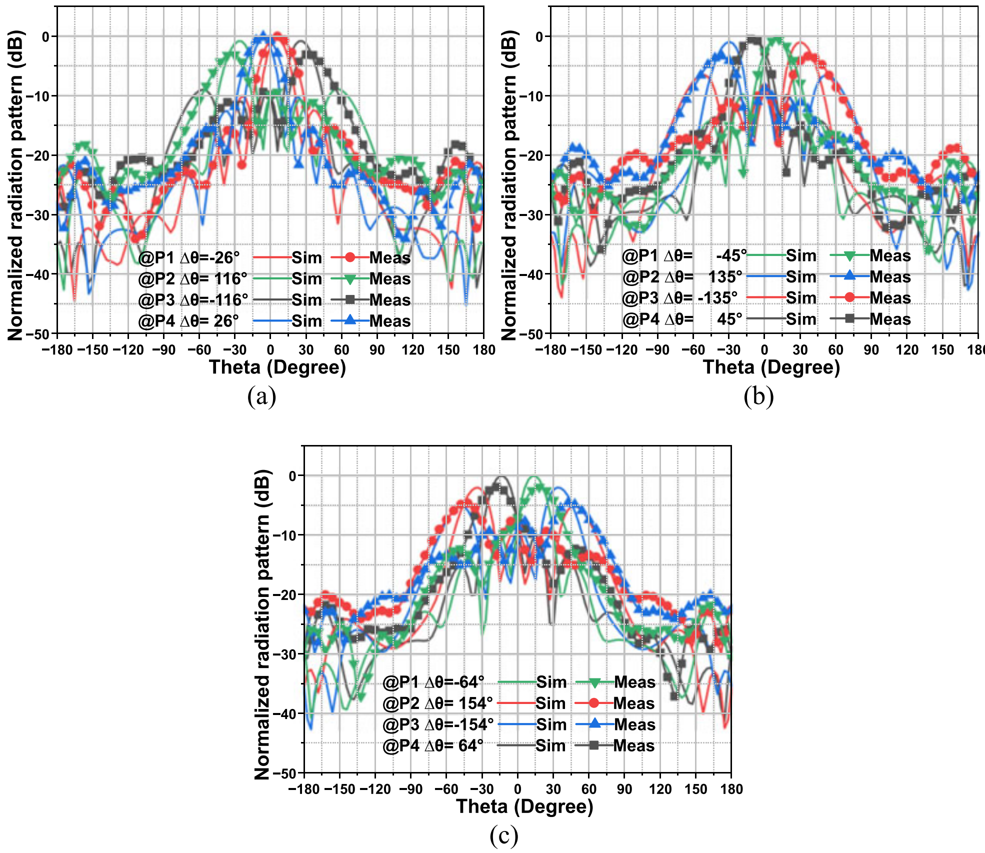

Figure 8. Simulated and measured radiation pattern: (a) Config_1, (b) Config_2, and (c) Config_3.

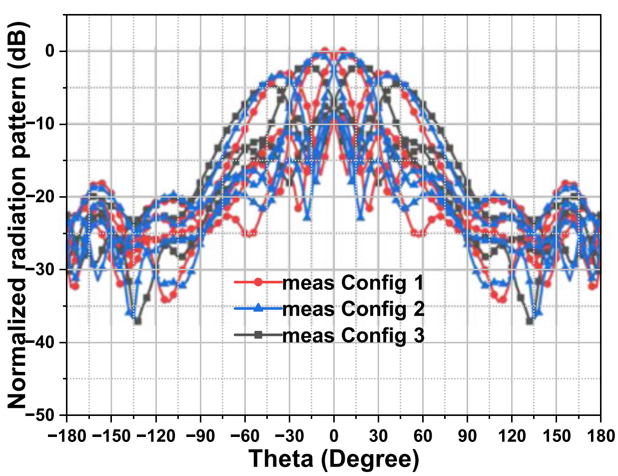

Figure 9. Measured radiation pattern of the three configurations.

Table 4. Comparison between the proposed Butler matrix with the state-of-the-art

	f_c (GHz)	Continuous tuning	Number of beams (4 × 4 Butler matrix)	Extra phase shifters	Feed loss
[12]	2.4	No	13 beams	Yes	1.7 dB
[14]	5.8	Yes	4 beams (beams are steered within a range from 18° to 30° depending on the excitation port)	Yes	<4 dB
[15]	2.4	No	8 beams	Yes	1.8 dB
[17]	2.4	No	12 beams	No	1.8 dB
This work	3.5	Yes	4 beams (each beam can be steered in a range of 12°)	No	1.7 dB (worse case)

When ports 1 and 4 are the input ports, the measured main beam is steered from $\pm 6^\circ$ to $\pm 18^\circ$ and from $\pm 32^\circ$ to $\pm 43^\circ$ when ports 2 and 3 are considered as input ports. A comparison with other relative Butler matrices is presented in Table 4. It is clear that the proposed BM has a continuously tunable phase difference when compared with the other proposals. Although in [14], the output phase difference is also continuously tunable, except that external phase shifters had to be added, resulting in increasing design area, which is directly related to the design cost and significant insertion losses compared to our proposed design.

Conclusion

A new concept of BM based on the conventional 4 × 4 structure is presented. This new concept demonstrates the feasibility of getting a continuous tunability of beams where it is not possible with the classical structure. The proposed Butler matrix is based on couplers with a tunable phase difference. To control the phase difference, each coupler requires four varactor diodes controlled by two bias voltages. Each of the four diodes of the couplers in the same row is fed by the same DC voltage. The proposed BM has been connected to an antenna array and then fabricated and tested. The prototype

https://doi.org/10.1017/S175907872300154X Published online by Cambridge University Press

has a simple structure and good radiation performance, capable of radiating four beams, where each beam can be steered in a range of 12°. With these results, the proposed system could become an attractive solution in beamforming and steering applications.

Acknowledgements. This work was supported by the Mobility support from Rennes Metropole, the European Union through the European Regional Development Fund, the French Ministry of Higher Education and Research, the Region Bretagne, the CPER Project 2015–2020 SOPHIE/STIC, and partly by Ondes.

Funding statement. This research received no specific grant from any funding agency, commercial, or not-for-profit sectors.

Competing interests. The authors report no conflict of interest.

References

1. **Blass J** (1960) Multidirectional antenna – A new approach to stacked beams. In *1958 IRE International Convention Record*, 48–50.
2. **Nolen J** (1965) Synthesis of multiple beam networks for arbitrary illuminations, Bendix Corporation, Radio Division.
3. **Butler J and Lowe R** (1961) Beam forming matrix simplifies design of electronically scanned antennas. *Electron Des* **9**, 170–173.
4. **Ali AAM, Fonseca NJG, Coccetti F and Aubert H** (2011) Design and implementation of two-layer compact wideband Butler matrices in SIW technology for Ku-band applications. *IEEE Transactions on Antennas and Propagation* **59**(2), 503–512.
5. **Zhang Y and Li Y** (2020) A dimension-reduction multibeam antenna scheme with dual integrated Butler matrix networks for low-complex massive MIMO systems. *IEEE Antennas and Wireless Propagation Letters* **19**(11), 1938–1942.
6. **Chang -C-C, Lee R-H and Shih T-Y** (2010) Design of a beam switching/steering Butler matrix for phased array system. *IEEE Transactions on Antennas and Propagation* **58**(2), 367–374.
7. **Ding K, He F, Ying X and Guan J** (2013) A compact 8×8 Butler matrix based on double-layer structure. In *2013 5th IEEE International Symposium on Microwave, Antenna, Propagation and EMC Technologies for Wireless Communications*, 650–653.
8. **Babale SA, Abdul Rahim SK, Barro OA, Himdi M and Khalily M** (2018) Single layered 4 × 4 Butler matrix without phase-shifters and crossovers. *IEEE Access* **6**, 77289–77298.
9. **Nedil M, Denidni TA and Talbi L** (2006) Novel Butler matrix using CPW multilayer technology. *IEEE Transactions on Microwave Theory & Techniques* **54**(1), 499–507.
10. **Wong YS, Zheng SY and Chan WS** (2012) Quasi-arbitrary phase-difference hybrid coupler. *IEEE Transactions on Microwave Theory & Techniques* **60**(6), 1530–1539.
11. **Wu Y, Shen J and Liu Y** (2013) Comments on "quasi-arbitrary phase-difference hybrid coupler". *IEEE Transactions on Microwave Theory & Techniques* **61**(4), 1725–1727.
12. **Chu HN and Ma T-G** (2018) An extended 4 × 4 Butler matrix with enhanced beam controllability and widened spatial coverage. *IEEE Transactions on Microwave Theory & Techniques* **66**(3), 1301–1311.
13. **Ma L, Wu Y and Wang W** (2021) Design of wideband Butler matrix with equal/unequal phase differences for flexible beam-controllability. *IEEE Transactions on Circuits and Systems II: Express Briefs* **68**(12), 3537–3541.
14. **Ren H, Li P, Gu Y and Arigong B** (2020) Phase shifter-relaxed and control-relaxed continuous steering multiple beamforming 4 × 4 Butler matrix phased array. *IEEE Transactions on Circuits and Systems I: Regular Papers* **67**(12), 5031–5039.
15. **Tajik A, Shafiei Alavijeh A and Fakharzadeh M** (2019) Asymmetrical 4 × 4 Butler matrix and its application for single layer 8 × 8 Butler matrix. *IEEE Transactions on Antennas and Propagation* **67**(8), 5372–5379.
16. **Ding K and Kishk A** (2017) Wideband hybrid coupler with electrically switchable phase-difference performance. *IEEE Microwave and Wireless Components Letters* **27**(11), 992–994.
17. **Ding K and Kishk AA** (2019) Extension of Butler matrix number of beams based on reconfigurable couplers. *IEEE Transactions on Antennas and Propagation* **67**(6), 3789–3796.
18. **Zhu H and Abbosh AM** (2018) A compact tunable directional coupler with continuously tuned differential phase. *IEEE Microwave and Wireless Components Letters* **28**(1), 19–21.
19. **Xu BW, Zheng SY and Long YL** (2019) A phase tunable hybrid coupler with enhanced bandwidth. *International Journal of RF and Microwave Computer-Aided Engineering* **29**(8), e21779.
20. **Pan YF, Zheng SY, Chan WS and Liu HW** (2020) Compact phase reconfigurable couplers with wide tuning range. *IEEE Transactions on Microwave Theory & Techniques* **68**(2), 681–692.
21. **Matthaei GL, Young L and Jones EMT** (1964) *Microwave Filters, Impedance Matching Networks and Coupling Structures*. New York: Mc Graw-Hill.
22. **M/A-COM Technology Solutions Inc. (MACOM)** MA46580 & MA46585 Beam Lead Constant Gamma GaAs Tuning Varactor, https://cdn.macom.com/datasheets/MA46580%20and%20MA46585.pdf

Taleb Mohamed Benaouf was born in Nouakchott, Mauritania, in 1991. He received the M.A.Sc. degree in Telecommunication Systems from the University El Manar of Tunis, Tunisia, in 2016. He is now pursuing the Ph.D. degree at the Mohammadia School of Engineering (EMI), Rabat, Morocco. His current research interests include reconfigurable circuit components, phased-array antennas, and millimeter-wave antenna array.

Abdelaziz Hamdoun was born in Zemamra, Morocco. He received the M.A.Sc. degree in Telecommunication Systems Engineering from the University of Rennes 1, Rennes, France, in 2012, and a co-joint Ph.D. degree in Electrical and Telecommunications Engineering in 2016 from both the Carleton University, Ottawa, Canada, and the University of Rennes 1, Rennes, France. He is currently working as an associate professor at the University of Poitiers. His research activities include the characterization and modeling of RF/microwave semiconductor devices based on GaN technology, the design of microwave integrated circuits in both GaN and CMOS technology, and the design of active frequency reconfigurable antennas and electronically beam forming antenna arrays.

Mohamed Himdi obtained his Ph.D. in Signal Processing and Telecommunications from the University of Rennes 1, France, in 1990. Since 2003, he has served as a professor at the University of Rennes 1 and led the High Frequency and Antenna Department at IETR until 2013. With a prolific publication record, he has authored or coauthored 163 journal papers and over 350 conference papers, boasting an H-index of 36. In addition, he has contributed to 12 book chapters and holds an impressive 46 patents. His research focus revolves around passive and active millimeter-wave antennas, encompassing the exploration of novel antenna array architectures and three-dimensional (3-D) antenna technologies. Recognized for his entrepreneurial spirit, he was honored as the Laureate of the 2nd National Competition for the Creation of Enterprises in Innovative Technologies in 2000 by the Ministry of Industry and Education. In March 2015, he received the JEC-AWARD in Paris for his work on a pure composite material antenna integrated into a motorhome roof, enhancing Digital Terrestrial Television reception. Further recognition came in 2021 when he was awarded the Innovation Trophy by the University of Rennes 1.

Olivier Lafond received the Ph.D. degree in Signal Processing and Telecommunications from the University of Rennes 1, Rennes, France, in 2000. Since October 2002, he has been an associate professor at the Institut d'Electronique et des Technologies du numéRique (IETR), University of Rennes. Since 2020, he has been a full professor at IETR. He has authored or coauthored 47 journal papers and 67 papers in conference proceedings. He has also authored/coauthored four book chapters. He holds eight patents in the area of antennas. His research activities concern passive and active millimeter-and submillimeter-wave antennas, quasi-optical systems (inhomogeneous lens), and plasma antennas. He has been responsible for one ESOA course since 10 years concerning millimeter-wave antennas.

Hassan Ammor is the Director of the Technological Innovation Center. Professor in the Department of Electrical Engineering at Mohammadia School of Engineering (EMI). He received his Ph.D. in Microwave Techniques from the Henry Poincaré University of Nancy in France in 1988 and Ph.D. in Applied Sciences from the Mohammadia School of Engineering in 1996 in Electronics Technology and Communications. He has authored over 120 technical papers in international journals and conferences. From 2005 to 2023, he has authored 15 scientific inventions. One of the inventions is an intelligent Moroccan scanner for the detection of breast cancer by microwave imaging. He has been awarded valuable prizes in research and innovation, including the Award of Merit and Medal at INPEX 2017, Pittsburgh, PA, USA; gold medal and Excellence Award at ICAN 2022 Inventors in Toronto, Canada; and four gold medals and the "Best Innovation Ecosystem" at IWA 2022. He is the author of the book "Techniques for measuring the complex permittivity of materials," European University Edition 2019.

https://doi.org/10.1017/S175907872300154X Published online by Cambridge University Press